

AD-A171 981

A DIFFERENTIAL SCANNING CALORIMETRY STUDY OF GUINIER
PRESTON ZONE FORMATI... (U) NAVAL AIR DEVELOPMENT CENTER
HARRINSTER PA AIRCRAFT AND CREW S... M FRAZIER
30 DEC 85 NADC-85169-60

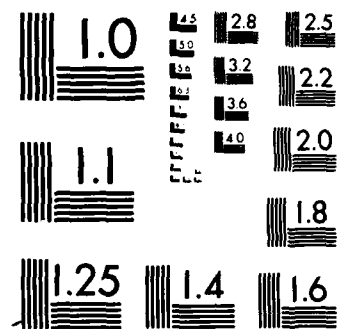
1/1

UNCLASSIFIED

F/G 11/6

NL





12



A DIFFERENTIAL SCANNING CALORIMETRY STUDY OF GUINIER PRESTON ZONE FORMATION AND DISSOLUTION IN 7075 AND 7091 ALUMINUM ALLOYS

William E. Frazier
Aircraft and Crew Systems Technology Directorate (Code 6063)
NAVAL AIR DEVELOPMENT CENTER
Warminster, PA 18974-5000

30 DECEMBER 1985

FINAL REPORT
Airtask No. A310310A/01B/4F61542000

Approved for Public Release. Distribution is Unlimited.

Prepared for
OFFICE OF NAVAL TECHNOLOGY
Department of the Navy
Washington, D.C. 20361

DTIC
ELECTE
SEP 16 1986
S E D

DTIC FILE COPY

AD-A171 881

NOTICES

REPORT NUMBERING SYSTEM - The numbering of technical project reports issued by the Naval Air Development Center is arranged for specific identification purposes. Each number consists of the Center acronym, the calendar year in which the number was assigned, the sequence number of the report within the specific calendar year, and the official 2-digit correspondence code of the Command Office or the Functional Directorate responsible for the report. For example, Report No. NADC-86015-20 indicates the fifteenth Center report for the year 1986, and prepared by the Systems Directorate. The numerical codes are as follows:

CODE	OFFICE OR DIRECTORATE
00	Commander, Naval Air Development Center
01	Technical Director, Naval Air Development Center
02	Comptroller
10	Directorate Command Projects
20	Systems Directorate
30	Sensors & Avionics Technology Directorate
40	Communications and Navigation Technology Directorate
50	Software Computer Directorate
60	Aircraft & Crew Systems Technology Directorate
70	Planning Assessment Resources
80	Engineering Support Group

PRODUCT ENDORSEMENT - The discussion or instructions concerning commercial products herein do not constitute an endorsement by the Government nor do they convey or imply the license or right to use such products.

APPROVED BY: 

J. S. GALLAGHER
CAPT, MSC, U.S. NAVY

DATE: 29 May 1986

UNCLASSIFIED

SECURITY CLASSIFICATION OF THIS PAGE

REPORT DOCUMENTATION PAGE

1a REPORT SECURITY CLASSIFICATION Unclassified		1b RESTRICTIVE MARKINGS AD-H177881	
2a SECURITY CLASSIFICATION AUTHORITY N/A		3 DISTRIBUTION AVAILABILITY OF REPORT Public Release	
2b DECLASSIFICATION DOWNGRADING SCHEDULE N/A			
4 PERFORMING ORGANIZATION REPORT NUMBER(S) NADC-85169-60		5 MONITORING ORGANIZATION REPORT NUMBER(S) N/A	
5a NAME OF PERFORMING ORGANIZATION Aircraft and Crew Systems Technology Directorate	6a OFFICE SYMBOL (If applicable) 6063	7a NAME OF MONITORING ORGANIZATION N/A	
5c ADDRESS (City, State, and ZIP Code) Naval Air Development Center Warminster, PA 18974-5000		7b ADDRESS (City, State, and ZIP Code) N/A	
8a NAME OF FUNDING SPONSORING ORGANIZATION Office of Naval Technology	8b OFFICE SYMBOL (If applicable) 225	9 PROCUREMENT INSTRUMENT IDENTIFICATION NUMBER N/A	
3c ADDRESS (City, State, and ZIP Code) Department of the Navy Washington, DC 20361		10 SOURCE OF FUNDING NUMBERS	
		PROGRAM ELEMENT NO See	PROJECT NO Reverse
		TASK NO Side	WORK UNIT ACCESSION NO
11 TITLE (Include Security Classification) A Differential Scanning Calorimetry Study of Guinier Preston Zone Formation and Dissolution in 7075 and 7091 Aluminum Alloys			
12 PERSONAL AUTHOR(S) William Frazier			
13a TYPE OF REPORT Final	13b TIME COVERED FROM _____ TO _____	14 DATE OF REPORT (Year, Month, Day) 1985 December 30	15 PAGE COUNT 20
16 SUPPLEMENTARY NOTES			
17 COSAT CODES		18 SUBJECT TERMS (Continue on reverse if necessary and identify by block number)	
FIELD	GROUP	SUB-GROUP	
		7091 Aluminum RST	
		Powder Metallurgy High Strength Aluminum	
		Extrusion	
19 ABSTRACT (Continue on reverse if necessary and identify by block number) The aging behavior of P/M 7091 and IM 7075 aluminum were studied by DSC; also hardness and conductivity. The energy associated with the formation and dissolution of Guinier Preston zones is correlated to mechanical and physical properties; equations for conductivity and hardness as a function of heat of reaction are presented. The activation energy for GP dissolution was established by differential scanning calorimetry (DSC) and values for ΔH^* , ΔG^* , and ΔS^* were calculated using absolute reaction rate theory. The activation energy calculated for GP dissolution in 7075-T6 is equivalent to the activation energy reported for the diffusion of Zn in aluminum.			
20 DISTRIBUTION AVAILABILITY OF ABSTRACT <input checked="" type="checkbox"/> UNCLASSIFIED UNLIMITED <input type="checkbox"/> SAME AS RPT <input type="checkbox"/> DTC USERS		21 ABSTRACT SECURITY CLASSIFICATION Unclassified	
22a NAME OF RESPONSIBLE NO. VOUAL William Frazier		22b TELEPHONE (Include Area Code) 22c OFFICE SYMBOL (215) 441-1301 6063	

TABLE OF CONTENTS

	Page
LIST OF TABLES.....	ii
LIST OF FIGURES.....	ii
INTRODUCTION.....	1
EXPERIMENTAL PROCEDURE.....	1
RESULTS.....	1
Interrelationship of Hardness, Conductivity and Heat of Reaction.....	2
Activation Energy for GP Zone Dissolution.....	2
Thermodynamic Potentials.....	3
DISCUSSION OF RESULTS.....	3
Conductivity.....	3
Free Energy of Activation.....	4
CONCLUSIONS.....	4
REFERENCES.....	5

Accession For	
NTIS GRA&I	<input checked="" type="checkbox"/>
DTIC TAB	<input type="checkbox"/>
Unannounced	<input type="checkbox"/>
Justification	
By _____	
Distribution/	
Availability Codes	
Dist	Avail and/or Special
A-1	



LIST OF TABLES

Table		Page
1	Thermodynamic Quantities of GP Zone Dissolution	6

LIST OF FIGURES

Figure		Page
1	DSC of Naturally Aged 7091 Aluminum Alloy	7
2	DSC of Naturally Aged 7075 Aluminum Alloy	8
3	DSC of 7075-T6 Aluminum Alloy.	9
4	DSC of 7091-T6 Aluminum Alloy.	10
5	Natural Aging Effect on the Heat of Reaction During GP Zone Formation/Dissolution	11
6	Hardness Profile of Naturally Aged 7091 and 7075 Aluminum Alloy	12
7	Conductivity Profile of Naturally Aged 7091 and 7075 Aluminum Alloy.	13
8	Linear Relationship Between the Heat of GP Dissolution, Conductivity, and Hardness in 7091 Aluminum Alloy.	14
9	Linear Relationship Between the Heat of GP Dissolution, Conductivity, and Hardness in 7075 Aluminum Alloy.	15
10	Thermal Data for GP Dissolution in 7091 Aluminum Alloy	16
11	Thermal Data for GP Dissolution in 7075 Aluminum Alloy	17
12	Thermal Data for GP Dissolution in 7075-T6 Aluminum Alloy.	18

INTRODUCTION

Aluminum 7075 and 7091 are two important precipitation hardening alloys. The precipitation process is complex and involves a series of interdependent steps. $SSS \rightarrow GP \rightarrow n'' \rightarrow n' \rightarrow n$; where SSS is the supersaturated solid solution, GP stands for Guinier Preston zones, n'' and n' are semi-coherent hexagonal precipitates of Mg and Zn, and n is the thermodynamically stable incoherent precipitate, $MgZn_2$. Differential scanning calorimetry (DSC) in conjunction with transmission electron microscopy (TEM) has been used to characterize the precipitate morphology (1, 2). A good correlation exists between DSC thermograms and the precipitation behavior of 7000 series alloys but models relating mechanical and physical properties to the DSC thermograms are lacking (3, 4).

Both 7075 and 7091 are used in two tempers: peak strength (T6) and overaged (T7). An essential part of the aging process involves a four day natural aging step which develops a homogeneous distribution of GP zones. The GP zones are extremely small clusters of Mg and Zn atoms. Those formed at room temperature are reported to be $20\text{-}30 \times 10^{-10}\text{m}$ in diameter. The GP zones are the nuclei from which the more stable precipitates can grow. The microstructure of the peak strength tempered aluminum has been reported to consist of 5% n' and 95% GP zones of $30\text{-}60 \times 10^{-10}\text{m}$ diameter with a density of 10^{12} GP/mm³ (5, 6). Thus, the GP zones represent the predominant precipitate in the T6 tempered material and make a significant contribution to the alloy's excellent mechanical properties.

This investigation centers on the formation and dissolution of GP zones during the natural aging process. DSC work was done in order to determine the stability of fully developed GP zones by establishing their activation energies for dissolution. GP zone formation was studied using DSC, electrical conductivity, and hardness measurements made at periodic intervals during the natural aging process. This permitted correlation to be made between heat of formation/dissolution, and the electrical conductivity and hardness response of these alloys.

EXPERIMENTAL PROCEDURE

Coupons of 7075 and 7091 ($1/2'' \times 1/2'' \times 1/4''$) were solutionitized at 482°C . for two hours and cold water quenched. Electrical conductivity was measured in units of %IACS (international annealed copper standard) using an eddy current conductivity meter. Both hardness (Rb) and conductivity were measured periodically during natural aging.

Thermal analysis was performed on a DuPont 1090 Thermal Analyzer employing a DSC module. Discs of 7075 and 7091 were heat treated in the same manner as the conductivity specimens. The power required to heat the 7075 and 7091 alloys was electronically subtracted from the power needed to heat a disc of pure aluminum of similar mass. Periodically during the aging process, DSC runs were performed at a heating rate of 10°C./min . Specimens naturally aged a minimum of 12 days were thermally analyzed at heating rates of 2, 10, and 20°C./min .

RESULTS

The results are divided into two categories: 1. the thermodynamic quantities for GP dissolution obtained for 7091 and 7075 naturally aged 12 days, and 2. the relationships between heat of reaction, electrical conductivity and hardness for naturally aged 7075 and 7091 aluminum.

The Differential Scanning Calorimetry (DSC) plots for 7075 and 7091 aged at room temperature are shown in Figures 1 and 2. The thermograms for 7075-T6 and 7091-T6 are shown in Figures 3 and 4. The graphs of the naturally aged material are divided into three regions: 1. GP formation/dissolution (50-150°C.), 2. n' formation/dissolution and n formation (150-280°C.), and 3. n dissolution (> 280°C.). (3,4) The term "heat of reaction" as used in this report refers to the area under the first peak occurring between 50-150°C. They are plotted in Figure 5. The curve has a sigmoidal shape initially positive, and as aging progresses becomes negative.

RELATIONSHIP BETWEEN HARDNESS, CONDUCTIVITY AND HEAT OF REACTION

The hardness vs. log time and conductivity vs. log time plots also appear sigmoidal. Upon naturally aging, hardness increased from R_B 40 to R_B 78 and conductivity decreased from 32 to 27% IACS as shown in Figures 6 and 7. Figures 8 and 9 show the conductivity and hardness data plotted against the heat of reaction. Both relationships appear linear, and regression analysis yields the following relationships:

7091

$$B = 1.41 \Delta H + 66.4 \quad (1)$$

$$s = 0.13 \Delta H + 28.29 \quad (2)$$

7095

$$B = 0.82 \Delta H + 67.2 \quad (3)$$

$$s = 0.13 \Delta H + 24.4 \quad (4)$$

Where B is hardness in R_B units:

s is electrical conductivity in % IACS

ΔH is the heat reaction in Jg⁻¹

The coefficient of correlation, r, is shown in each figure.

ACTIVATION ENERGY FOR GP ZONE DISSOLUTION

The activation energies for GP dissolution were determined, according to ASTM E 698-79 (6) by determining the slope of log β vs. 1/T as shown in Figure 10, 11, and 12. The slope was calculated by a regression analysis where β is heating rate in °C. min.⁻¹ and T is the peak temperature in K. The peak temperature is that temperature where the reaction rate is maximum.

The activation energy (E*) was calculated using:

$$(\text{ref. 7}) E^* = 2.19R \frac{\Delta \log \beta}{\Delta (1/T)} \quad (5)$$

The value of E* was refined by using an iterative technique presented in ref. 6. The specific rate constant can be calculated by:

$$k = k_0 \exp \frac{[-E^*]}{RT} \quad (6)$$

Where the term k_0 is given by:

$$k_0 = B E^* \exp \frac{[E^*]}{RT} (RT^2)^{-1} \quad (7)$$

THERMODYNAMIC POTENTIALS

From absolute reaction rate theory,

$$K = \frac{RT \exp(-\Delta G)}{hN} = \frac{RT \exp(-\Delta H) \exp \frac{(\Delta S)}{R}}{hN} \quad (8)$$

where

R is the universal constant

h is Plank's constant

N is Avogadro's number

Rearranging equations 6, 7, and 8 produces (ref. 3)

$$\Delta H = E - RT \quad (9)$$

$$\Delta G = RT \ln \frac{(KhN)}{RT} \quad (10)$$

$$\Delta S = \frac{(\Delta G - \Delta H)}{T} \quad (11)$$

The value of ΔG , ΔH , ΔS , and E are presented in Table 1. The free energy of activation of 7091 and 7095 naturally aged and in the T6 condition are similar; the value of ΔG for the dissolution of GP zones in the T6 temper is at $130.9 \text{ KJ mol}^{-1}$ substantially higher, reflecting its greater strength and higher thermal stability of the precipitate formed during artificial aging.

DISCUSSION OF RESULTS

Mechanical and physical properties depend a great deal on the microstructure of an alloy. Supersaturated solid solutions, obtained by rapid quenching from solution heat treatment temperatures, generally have low electrical conductivity and are soft compared to age hardened aluminum. The increase in yield strength and hardness during natural aging is directly related to the precipitation of coherent/semicoherent particles.

CONDUCTIVITY

Classical physical metallurgy principles state that electrical conductivity should increase during aging since solute atoms are removed from the matrix. In this study, 7075 and 7091 alloys exhibit a decrease in conductivity with natural aging commonly called "the resistivity maximum". This is a consequence of the complex precipitation process. During room temperature aging, only a fraction of the solute is removed from the matrix, perhaps not enough to significantly increase conductivity. The GP zones that precipitate are of a size and distribution that interferes with the standing waves of the conduction band electrons. The GP zones formed have significant strain

fields and these apparently contribute more toward impeding electron movement than does the decrease matrix solute to increase electron mobility, hence, decreased electrical conductivity.

This study has shown electrical conductivity and hardness to be functions of the heat of reaction. This appears reasonable, since during mechanical deformation processes energy is required to pass dislocations through the material, breaking atomic bonds; and the heat of reaction is a measure of the quantity and stability of the strengthening precipitates. During the initial few minutes of natural aging, few GP zones have nucleated, and so the material's resistance to deformation is small. A DSC thermogram made at this time yields a large exothermic peak corresponding to GP zone nucleation (Figures 1 and 2). After several thousand hours of natural aging, the majority of GP zones have nucleated and grown. These zones then provide a great deal of resistance to dislocation motion and require thermal energy to dissolve. This absorption corresponds to the endothermic peaks on the DSC thermographs of Figures 1 and 2.

FREE ENERGY OF ACTIVATION

The GP zones formed at room temperature in 7075 and 7091 have similar free energies of activation: 107 KJ mol^{-1} . The entropy contribution to the free energy of activation is slightly larger for 7091 than it is for 7075 (Table 1). Aging 7075 and 7091 to the T6 condition stabilizes the GP zones. This is reflected by the increase in free energy of activation from 106 to 131 KJ mol^{-1} . This value corresponds well with the value of 137 KJ mol^{-1} previously reported (2).

The activation energy calculated for GP dissolution in 7075 is 119 KJ mol^{-1} . This figure compares well with the reported value of the activation energy for the diffusion of Zn in aluminum, 120 KJ mol^{-1} (7). This is reasonable since Zn is a major constituent of the precipitated phase.

CONCLUSIONS

1. The heat of reaction for GP zone formation/dissolution as determined by DSC analysis is linearly related to hardness and electrical conductivity.
2. Conductivity decreases with room temperature aging due to the formation of GP zones.
3. The free energy of activation for 7075 and 7091 are similar when naturally and artificially aged.
4. The activation energy for GP zone dissolution in 7075-T6 is similar to the activation energy for the diffusion of zinc in aluminum.

REFERENCES

1. J. Papazian, "Calorimetric Studies of Precipitation and Dissolution Kinetics in Aluminum Alloys 2219 and 7075," Met. Trans. A, 13A, May, 1982.
2. P. Adler and R. Delasi, "Calorimetric Studies of 7000 Series Aluminum Alloys: 11 Comparisons of 7075, 7050, and RX720 Alloys," Met. Trans. A, 8A, July 1977, p. 1185.
3. J. Papazian, "Effect of Two-Stage Aging on the Microstructure of 7075 Aluminum Alloys," Grumman Aerospace, April, 1981, N00019-79-C-0285.
4. D. Skinner, R. Kerr, M. Koczak and A. Lawley, "Aging Response of a High Strength PM Aluminum Alloy," Drexel University.
5. G.W. Lorimer, "Precipitation in Aluminum Alloys," Precipitation Process in Solids, Conf. Proc. AIME (Ed. K.C. Russell and H.I. Ahronson), 1976.
6. ASTM, "Arrhenius Kinetic Constants for Thermally Unstable Materials," ASTM E-698-79.
7. Handbook of Chemistry and Physics, 62nd Ed. CRC, 1981-83.

TABLE 1

THERMODYNAMIC QUANTITIES FOR G.P. ZONE DISSOLUTION

<u>Alloy</u>	<u>ΔG^* (KJ mol⁻¹)</u>	<u>ΔH^* (KJ mol⁻¹)</u>	<u>ΔS^* (J mol⁻¹ K⁻¹)</u>	<u>E^* (KJ mol⁻¹)</u>
7075-T6	130.9	115	-34.2	119
7075 - Nat. Aged	106.0	92.3	-36.5	95.4
7091 - Nat. Aged	106.1	87.1	-50.8	90.2

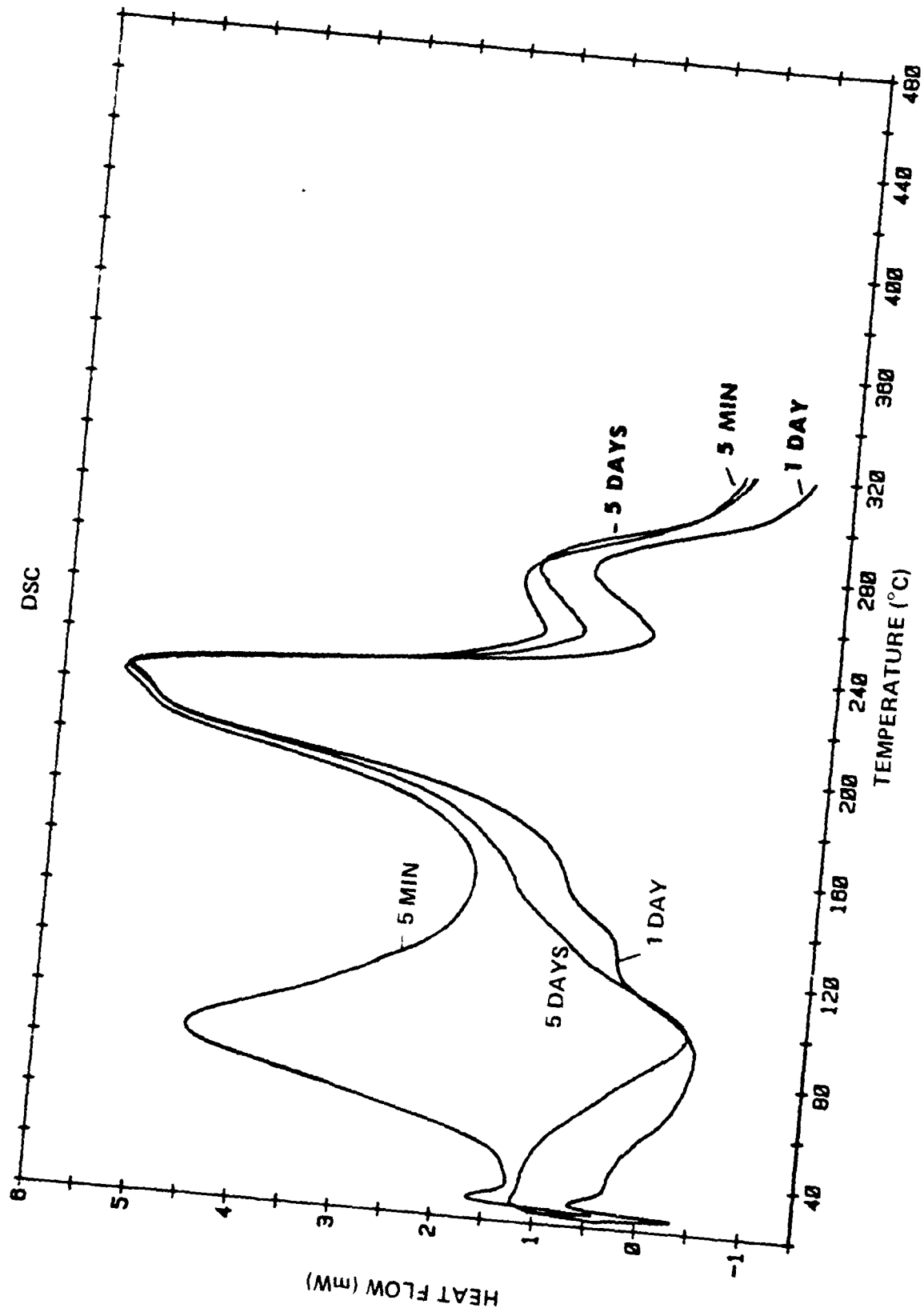


Figure 1. DSC of Naturally Aged 7091 Aluminum Alloy

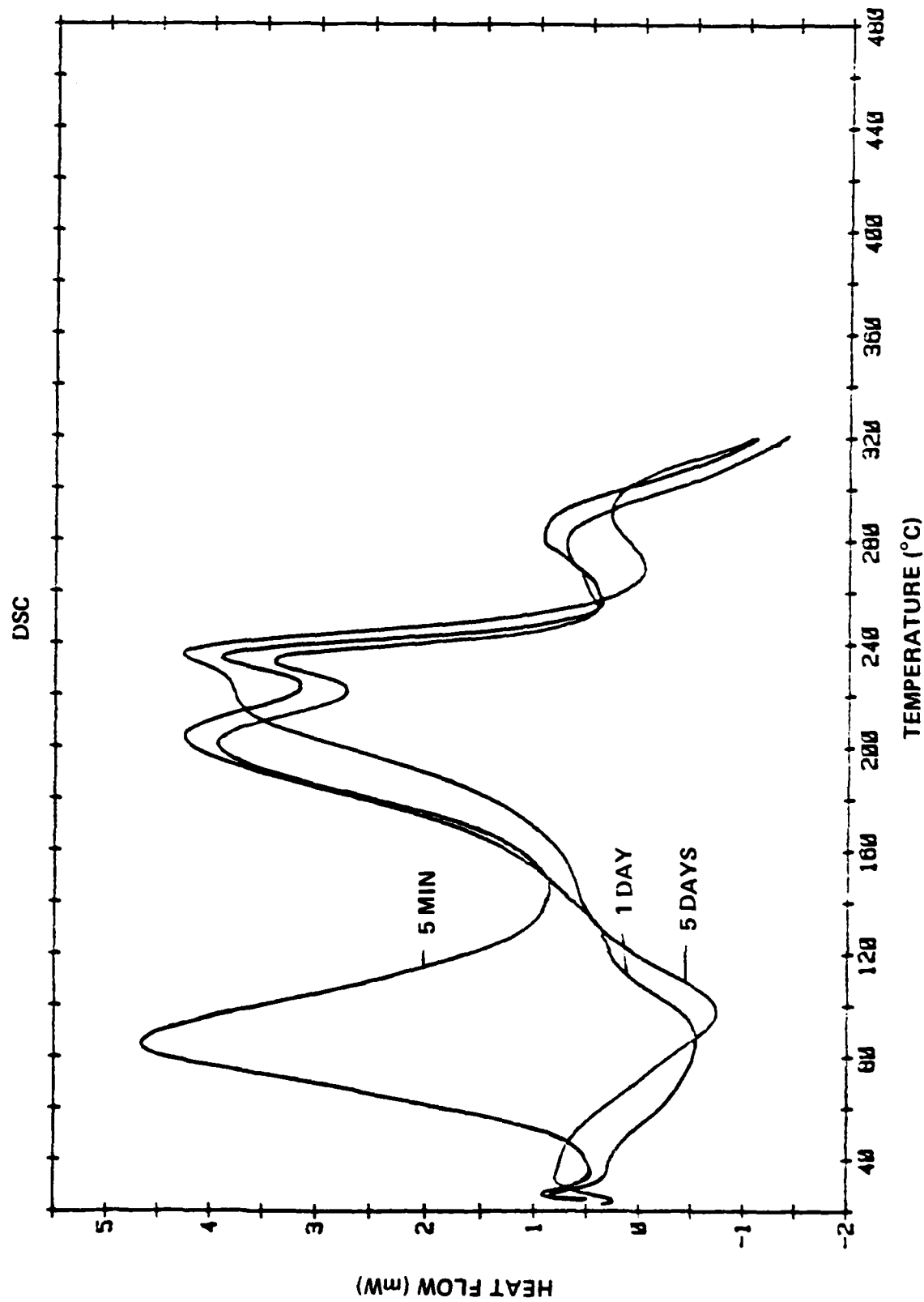


Figure 2. DSC of Naturally Aged 7075 Aluminum Alloy

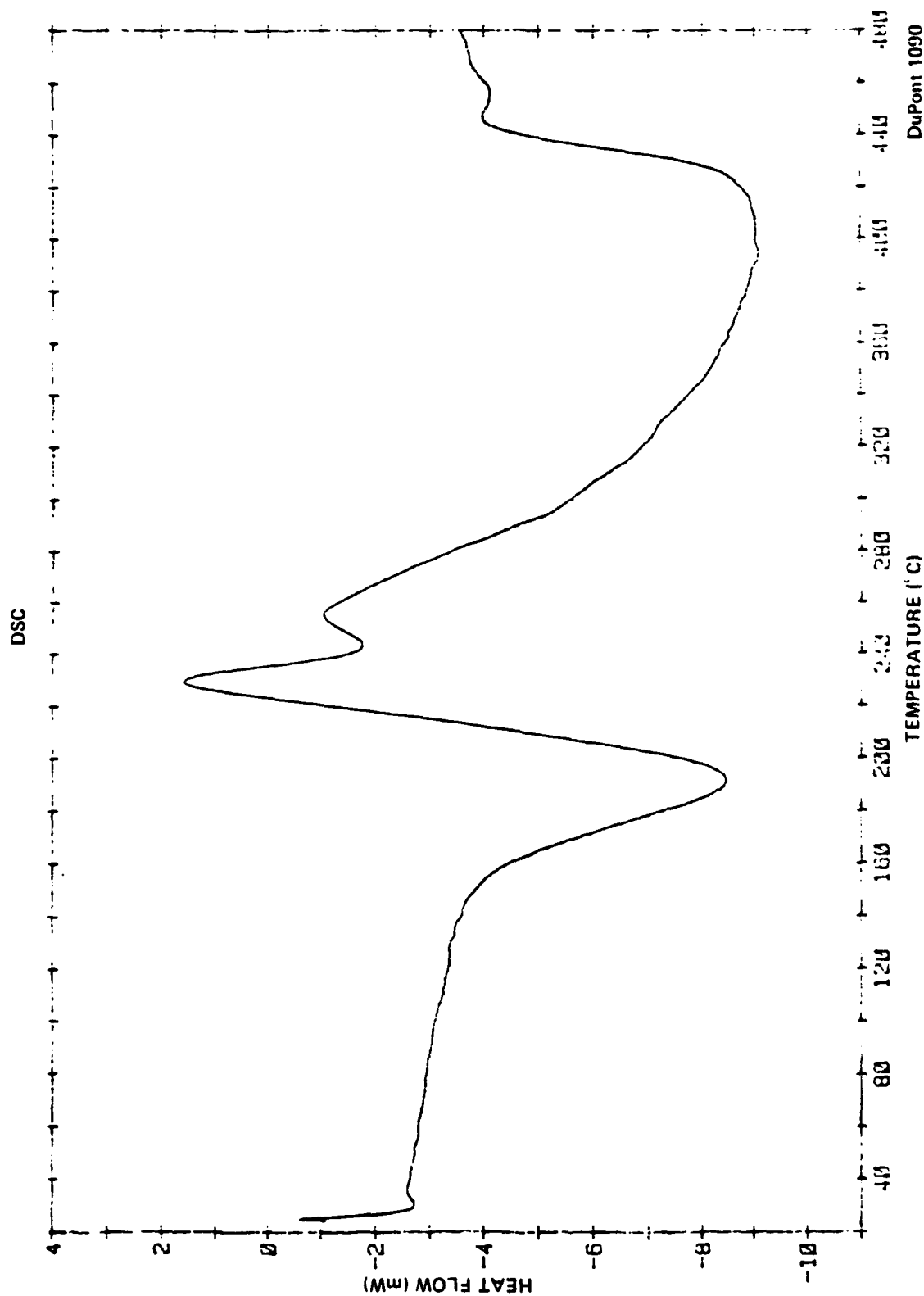


Figure 3. DSC of 7075-T6 Aluminum Alloy

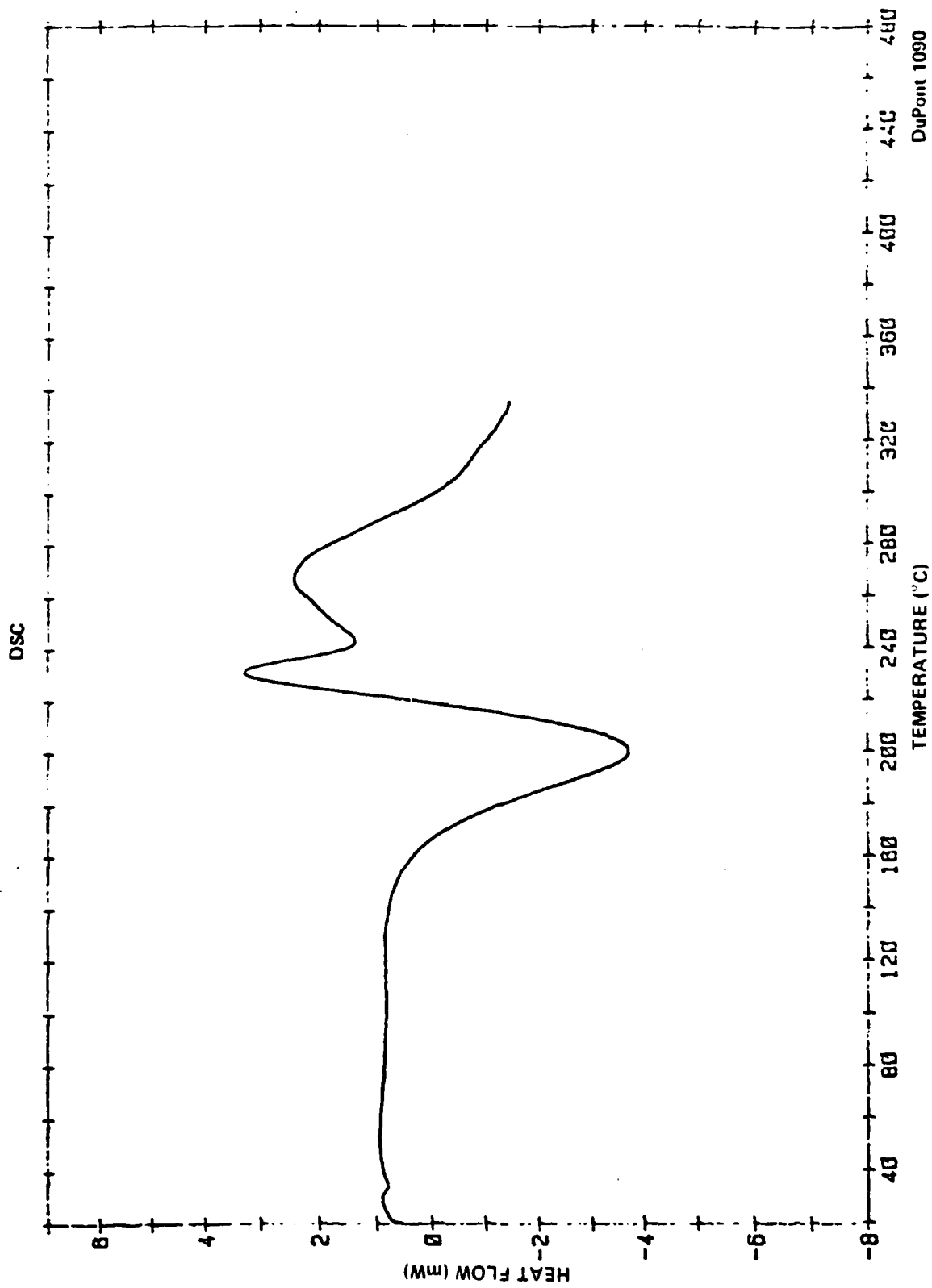


Figure 4. DSC of 7091-T6 Aluminum Alloy

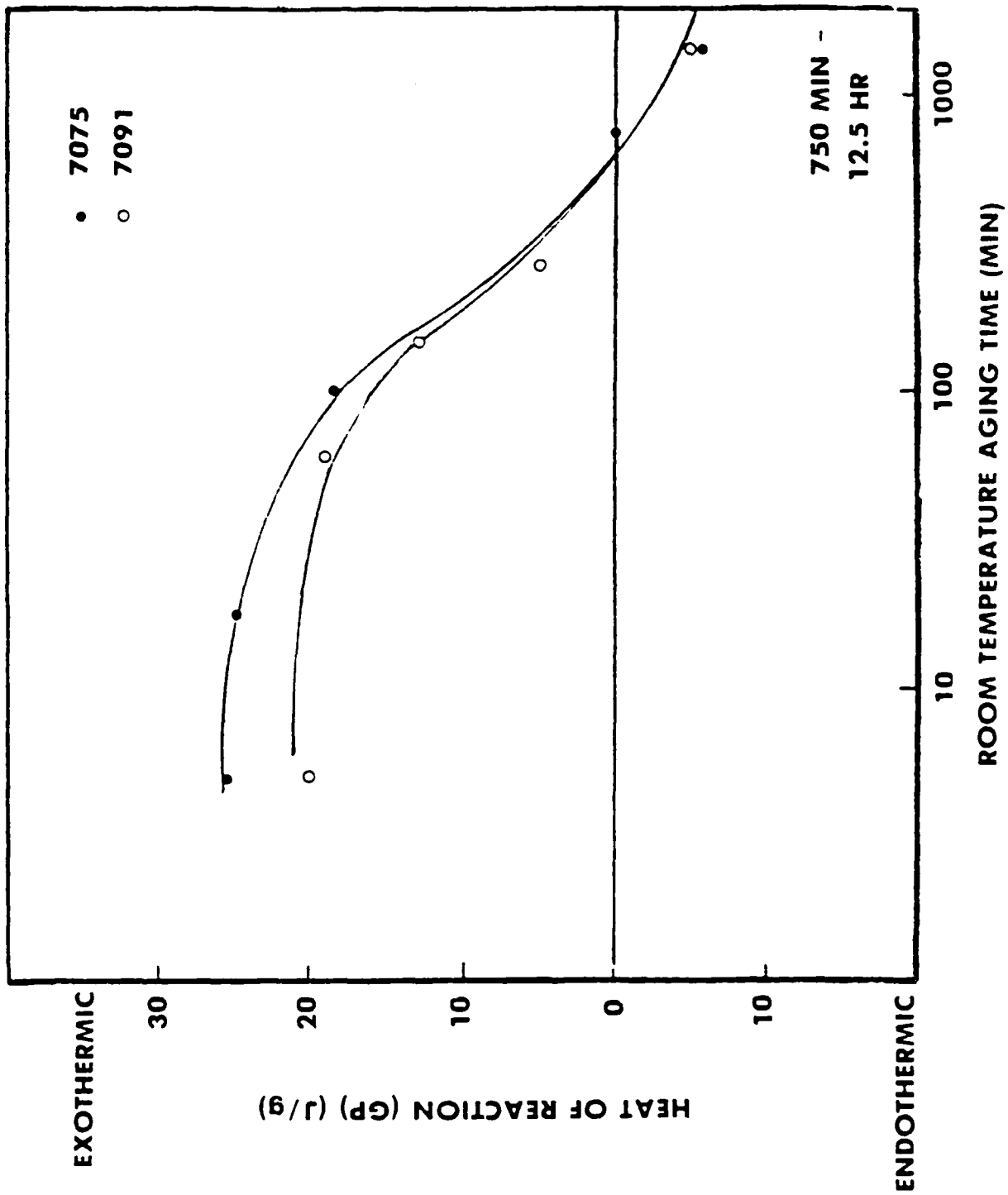


Figure 5. Naturally Aging Effect on the Heat Reaction During GP Zone Formation Dissolution

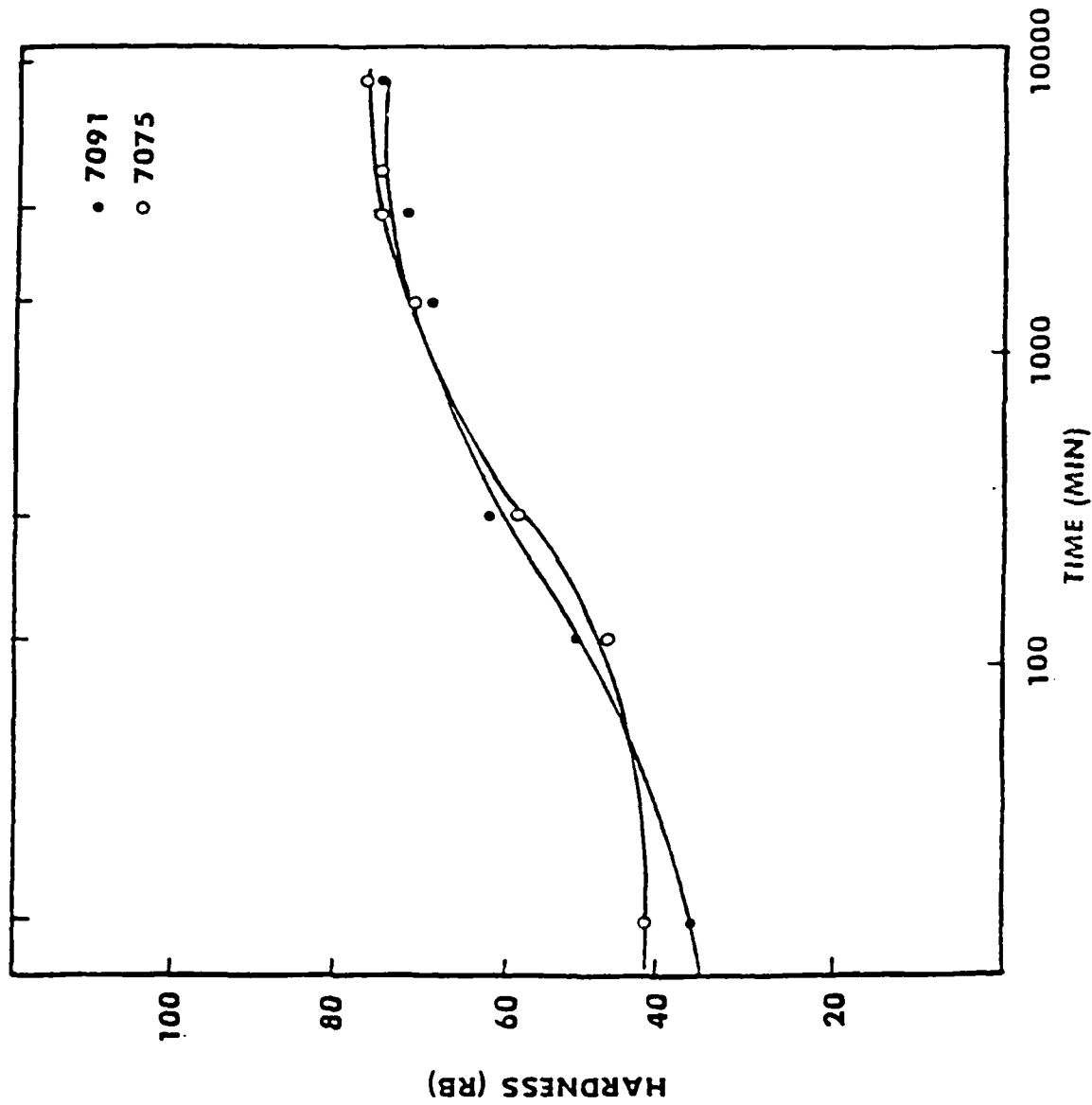


Figure 6. Hardness Profile of Naturally Aged 7091 and 7075 Aluminum Alloy

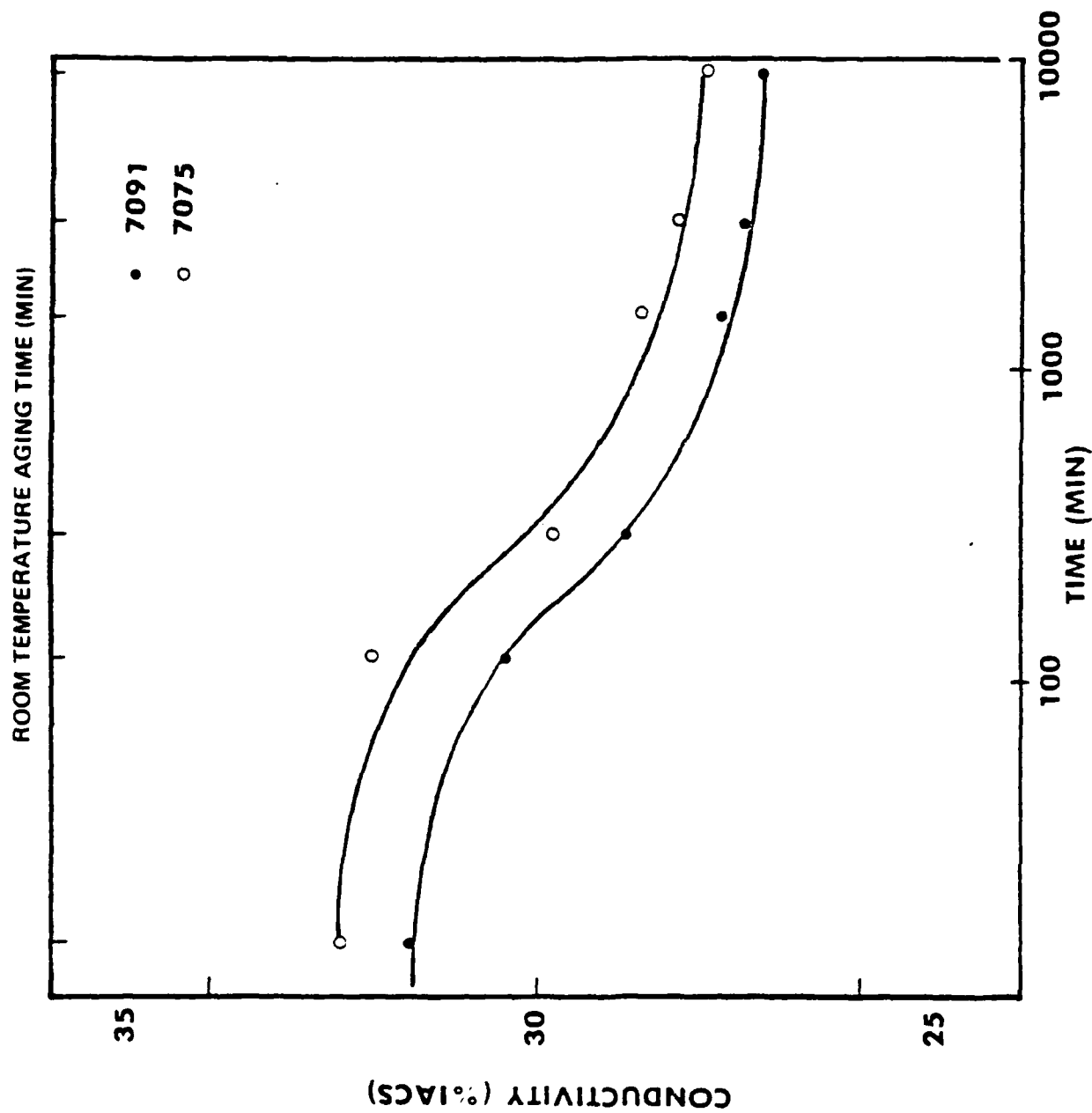


Figure 7. Conductivity Profile of Naturally Aged 7091 and 7075 Aluminum Alloy

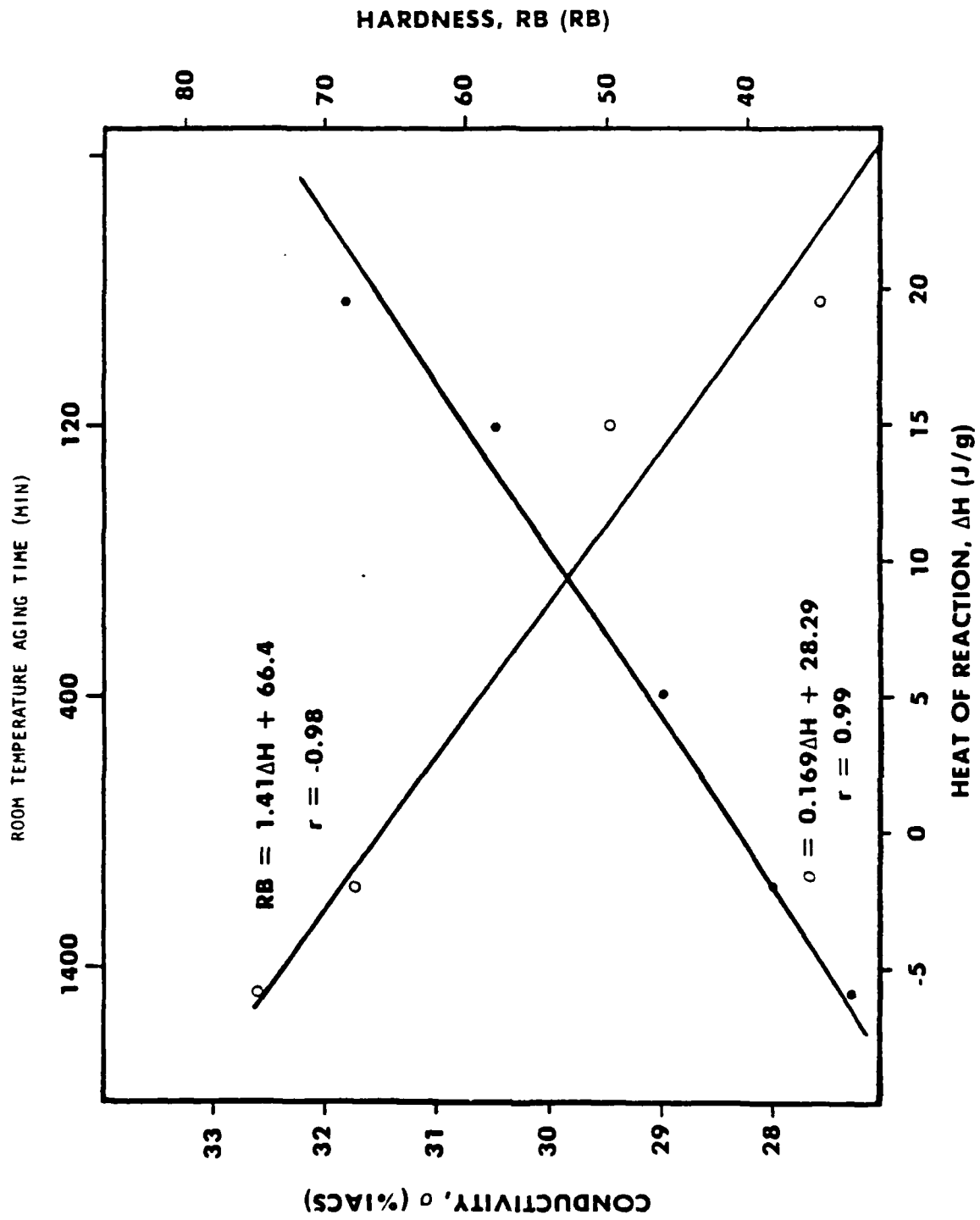


Figure 8. Linear Relationship Between the Heat of GP Dissolution, Conductivity and Hardness in 7091 Aluminum

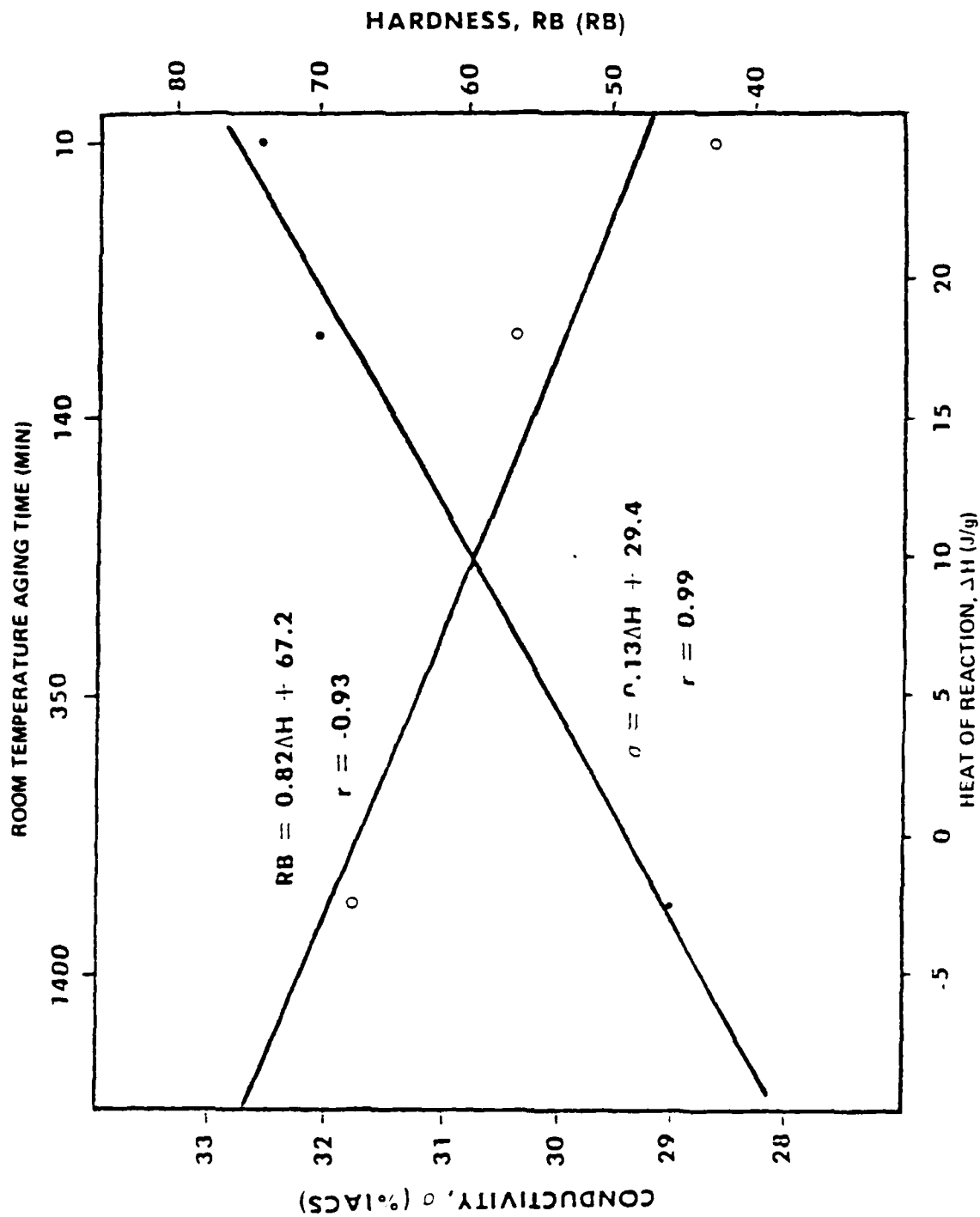


Figure 9. Linear Relationship Between the Heat of GP Dissolution, Conductivity and Hardness of 7075 Aluminum

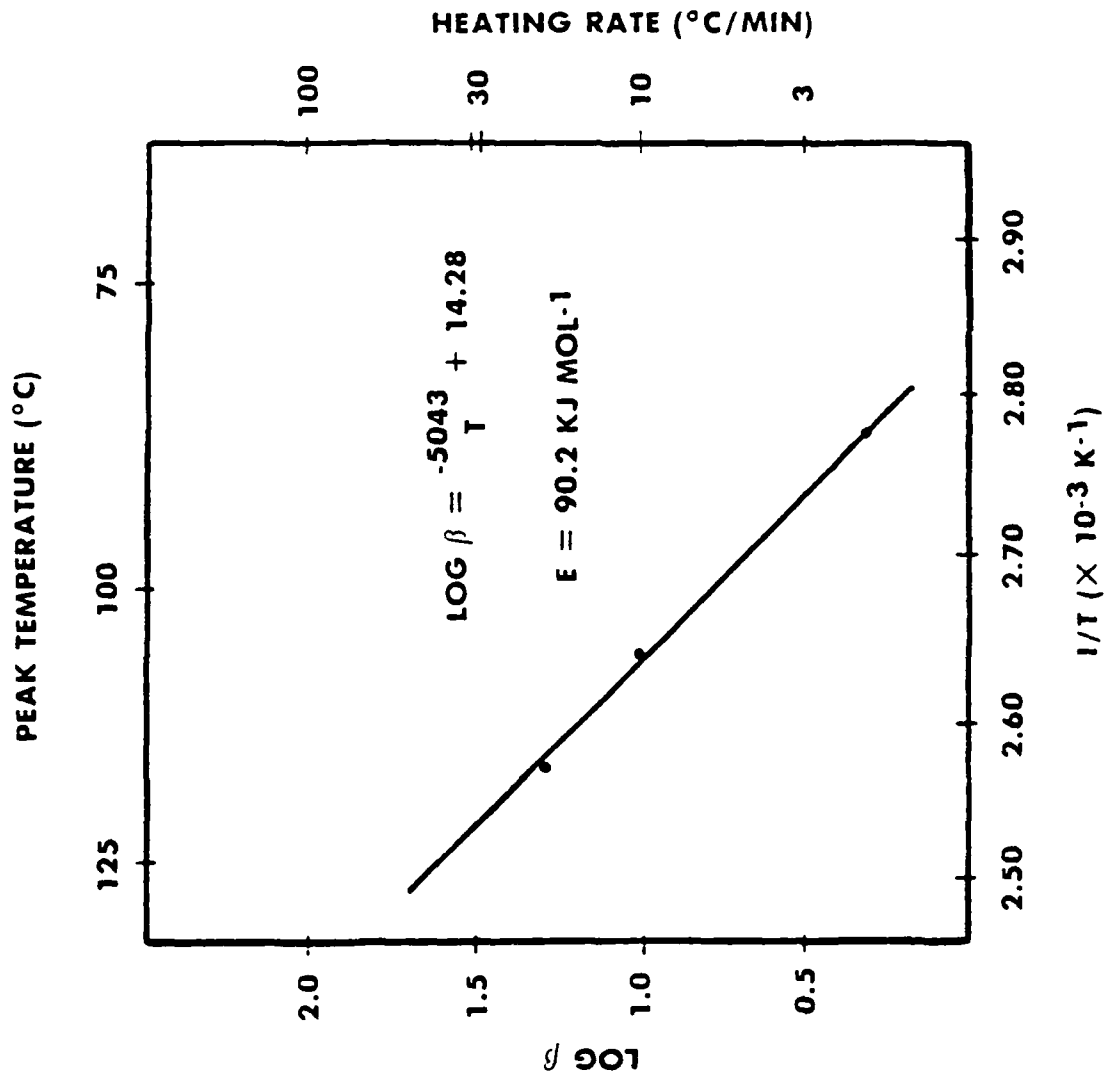


Figure 10. Thermal Data for GP Dissolution in 7091 Aluminum

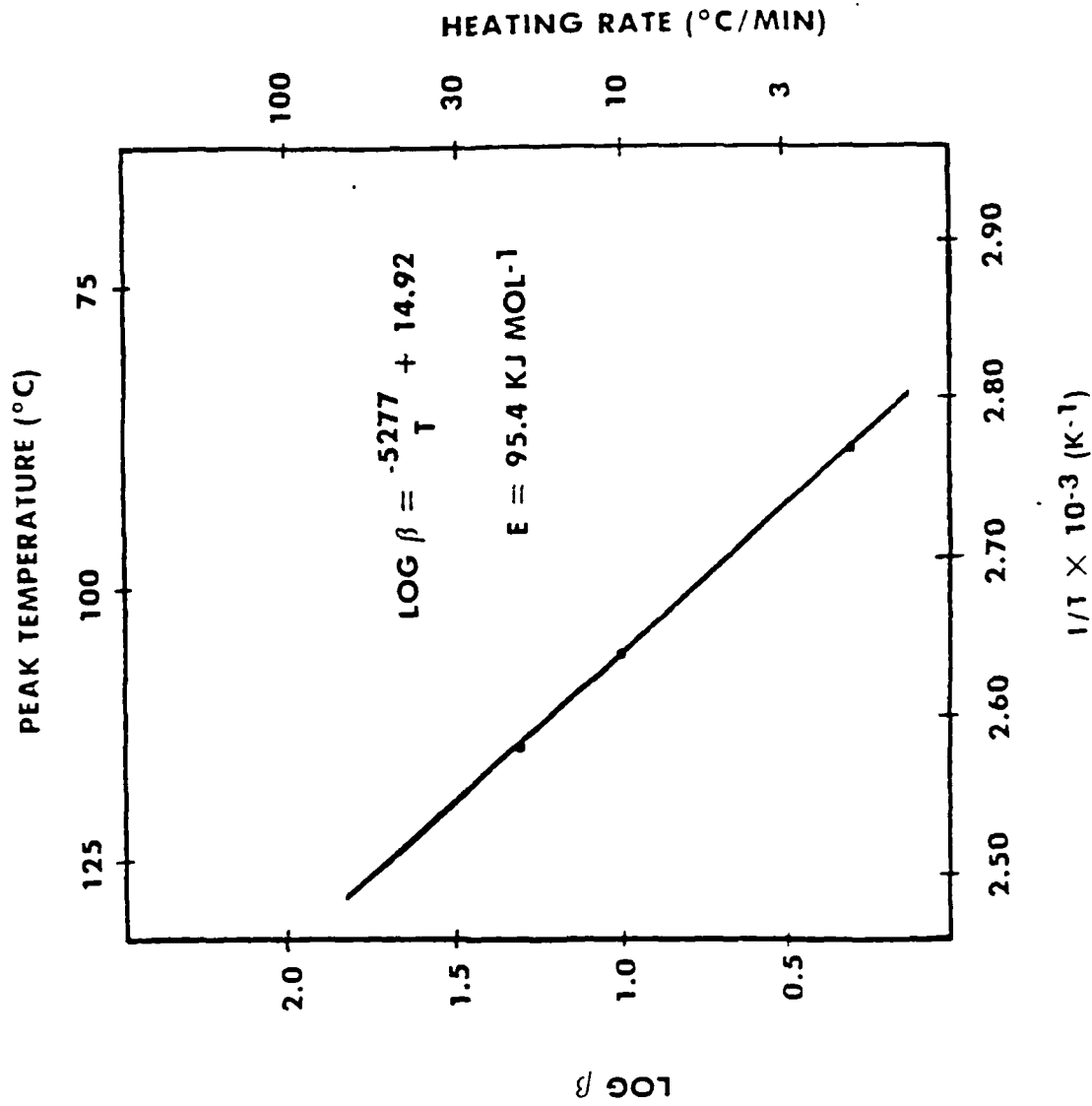


Figure 11. Thermal Data for GP Dissolution in 7075 Aluminum Alloy

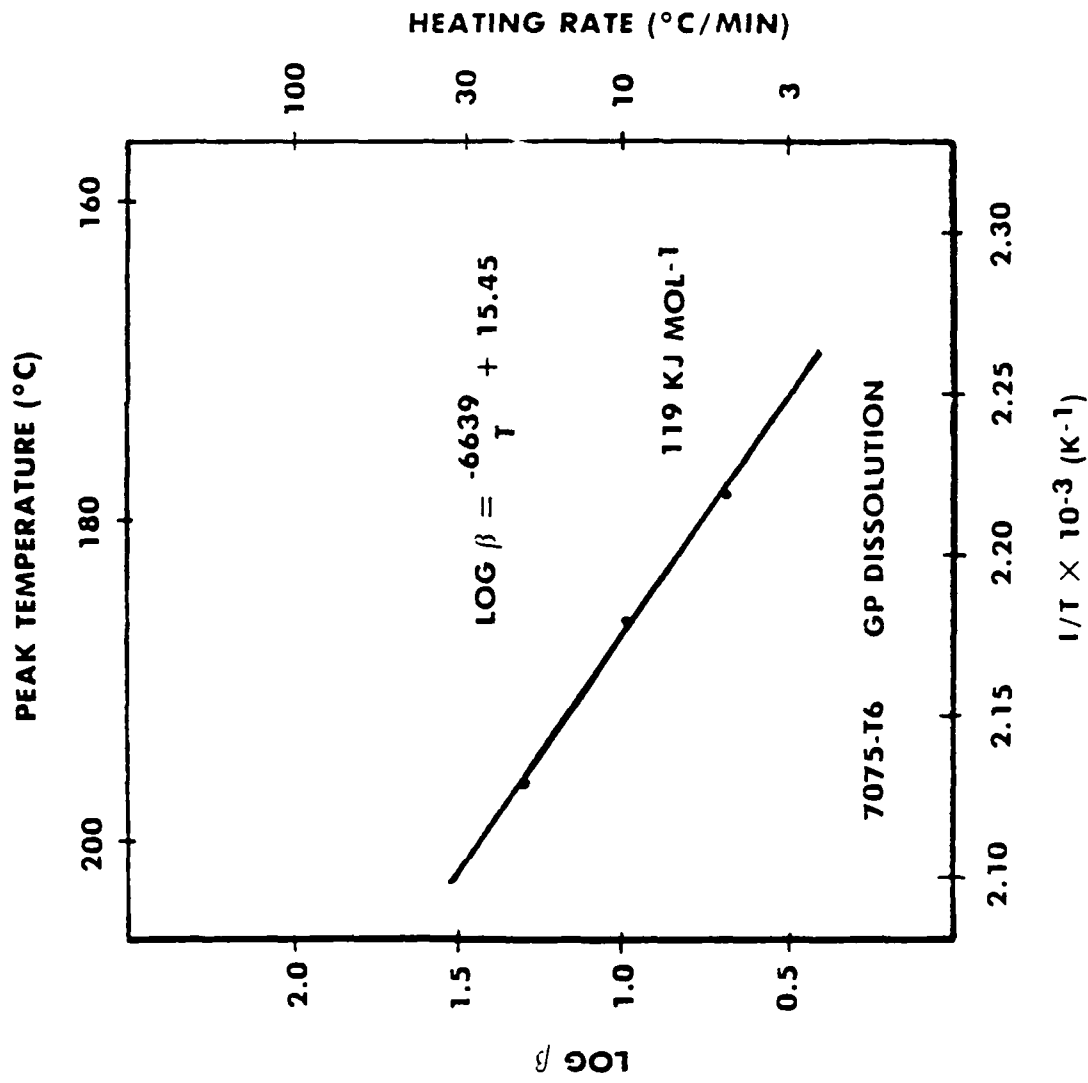


Figure 12. Thermal Data for GP Dissolution in 7075 T6 Aluminum Alloy

END

10-86

DTIC